Magn. Reson., 2, 139–148, 2021
https://doi.org/10.5194/mr-2-139-2021

Open Access
MAGNETIC
RESONANCE

Exchange interaction in short-lived flavine adenine dinucleotide biradical in aqueous solution revisited by CIDNP (chemically induced dynamic nuclear polarization) and nuclear magnetic relaxation dispersion

Ivan V. Zhukov[1,2], Alexey S. Kiryutin[1,2], Mikhail S. Panov[1,2], Natalya N. Fishman[1,2], Olga B. Morozova[1,2], Nikita N. Lukzen[1,2], Konstantin L. Ivanov[1,2,†], Hans-Martin Vieth[1,3], Renad Z. Sagdeev[1,2], and Alexandra V. Yurkovskaya[1,2]

[1]International Tomography Center, Siberian Branch of the Russian Academy of Sciences, Novosibirsk, 630090, Russia
[2]Department of Natural Sciences, Novosibirsk State University, Novosibirsk, 630090, Russia
[3]Institut für Experimentalphysik, Freie Universität Berlin, 14195 Berlin, Germany
[†]deceased, 5 March 2021

Correspondence: Alexandra V. Yurkovskaya (yurk@tomo.nsc.ru)

Received: 5 February 2021 – Discussion started: 16 February 2021
Revised: 24 March 2021 – Accepted: 29 March 2021 – Published: 13 April 2021

Abstract. Flavin adenine dinucleotide (FAD) is an important cofactor in many light-sensitive enzymes. The role of the adenine moiety of FAD in light-induced electron transfer was obscured, because it involves an adenine radical, which is short-lived with a weak chromophore. However, an intramolecular electron transfer from adenine to flavin was revealed several years ago by Robert Kaptein by using chemically induced dynamic nuclear polarization (CIDNP). The question of whether one or two types of biradicals of FAD in aqueous solution are formed stays unresolved so far. In the present work, we revisited the CIDNP study of FAD using a robust mechanical sample shuttling setup covering a wide magnetic field range with sample illumination by a light-emitting diode. Also, a cost efficient fast field cycling apparatus with high spectral resolution detection up to 16.4 T for nuclear magnetic relaxation dispersion studies was built based on a 700 MHz NMR spectrometer. Site-specific proton relaxation dispersion data for FAD show a strong restriction of the relative motion of its isoalloxazine and adenine rings with coincident correlation times for adenine, flavin, and their ribityl phosphate linker. This finding is consistent with the assumption that the molecular structure of FAD is rigid and compact. The structure with close proximity of the isoalloxazine and purine moieties is favorable for reversible light-induced intramolecular electron transfer from adenine to triplet excited flavin with formation of a transient spin-correlated triplet biradical $F^{\bullet -}$-$A^{\bullet +}$. Spin-selective recombination of the biradical leads to the formation of CIDNP with a common emissive maximum at 4.0 mT detected for adenine and flavin protons. Careful correction of the CIDNP data for relaxation losses during sample shuttling shows that only a single maximum of CIDNP is formed in the magnetic field range from 0.1 mT to 9 T; thus, only one type of FAD biradical is detectable. Modeling of the CIDNP field dependence provides good agreement with the experimental data for a normal distance distribution between the two radical centers around 0.89 nm and an effective electron exchange interaction of −2.0 mT.

Published by Copernicus Publications on behalf of the Groupement AMPERE.

1 Introduction

Flavins play an important role as coenzymes in various biological systems and therefore have been studied extensively. Thus, the optical absorption and fluorescence properties of ground state, excited states, and various free-radical forms have been well characterized. Flavin adenine dinucleotide (FAD) attracted much attention in the last decades as a cofactor of the cryptochrome photoreceptor that is suggested to be responsible for sensitivity to the Earth's magnetic field in animal and avian navigation (Wiltschko and Wiltschko, 2019). A review on the radical-pair mechanism (RPM) of magnetoreception as a leading hypothesis to explain bird navigation can be found in the literature (Hore and Mouritsen, 2016). The same mechanism of photocycle and signaling action of plant cryptochrome in Arabidopsis was reviewed recently (Ahmad, 2016). The keystone of the proposed explanation is as follows: the blue-light-activated flavin moiety of FAD oxidizes a chain of three tryptophan compounds resulting in a radical pair composed of a singly reduced semiquinone flavin and an oxidized tryptophan. Accordingly, the singlet/triplet spin dynamics of the FAD^{-}/Trp^{+} radical pair have been intensively studied as the source of cryptochrome sensitivity to the Earth's magnetic field.

In all these studies, the role of adenine was obscure or limited to the role of a binding site to the protein, but interaction between the photo-excited flavin and adenine was neglected. As a result, the light-induced reaction of intramolecular electron transfer between the two FAD moieties was not considered, presumably because the adenine radical is a weak chromophore, being hardly detectable by optical methods (Murakami et al., 2005; Antill and Woodward, 2018). To the best of our knowledge, the influence of the flavin–adenine biradical on the magnetic field dependence of transient absorption was not taken into consideration by a large scientific community, probably because most of their studies were based on various optical methods. However, as it was shown by Robert Kaptein and co-workers (Stob et al., 1989), upon light excitation of the flavin moiety of FAD, a short-lived triplet biradical is formed by intramolecular electron transfer from the adenine (see Scheme 1).

In that breakthrough study, Kaptein applied chemically induced dynamic nuclear polarization (CIDNP), being a sensitive tool for magnetic resonance characterization of short-lived radicals that are too elusive for EPR detection or do not have a suitable optical band. In Kaptein's work (Stob et al., 1989), CIDNP effects arising from the FAD biradical were reported at high and low magnetic field under continuous light illumination. In the field dependence of emissive nuclear polarization, two contributions were discerned with the maxima at 3.0 and 10.0 mT, respectively. Strong electronic exchange interaction was revealed, much higher than the Earth's field. This type of interaction splits the singlet and triplet states of the biradical and leads to a CIDNP maximum at the level anti-crossing of one of the triplet electronic

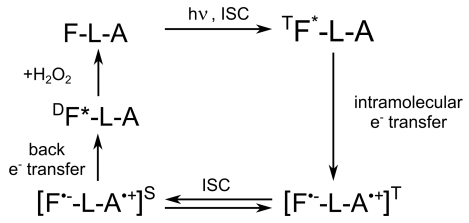

Scheme 1. Cyclic photochemical reaction of reversible intramolecular electron transfer from adenine to flavin in FAD molecules in aqueous solution. The triplet–singlet transition in the short-lived flavin–adenine biradical leads to formation of CIDNP. The FAD molecule is shown as F-L-A, where F denotes flavin, L denotes the ribityl phosphate linker, and A denotes adenine.

states $T_{\pm}$ with S. The presence of avoided level crossings in the primary biradical is encoded in the magnetic field dependence of the reaction yield and, in general, in the lifetime of the flavin radical. Often FAD is discussed as a candidate molecule responsible for the formation of such spin-correlated radical pairs in living organisms that contain particular proteins – blue-light photoreceptors, cryptochromes, which contain a non-covalently bound FAD photoreceptor molecule. The radical pair usually considered is a pair of radicals $[FAD^{\bullet-}\ Trp^{\bullet+}]$, which is formed by sequential electron transfer along the chain of tryptophan residues to the cofactor FAD in cryptochrome (Dodson et al., 2015). However, the appearance of the magnetic field effect in this secondary radical pair, $[FAD^{\bullet-}\ Trp^{\bullet+}]$, formed in parallel or subsequently from the FAD biradical, might be significantly affected by the spin dynamics in the primary FAD biradical.

Let us briefly explain the mechanisms of such nuclear spin polarization formation in transient radical pairs or biradicals with nonzero exchange interaction. For simplicity, we consider the case of a biradical with only one spin-1/2 nucleus and an exchange interaction much larger than the hyperfine coupling (HFC) with that single nucleus. A distinct maximum ("J resonance") of nuclear polarization in the vicinity of the level crossing (LC) between the electronic singlet and one of the triplet states (T_+ or T_- for positive or negative J, respectively) of the biradical is detected by NMR in the diamagnetic products. The reason is that nonsecular terms of HFC induce transitions conserving the z projection of the total spin of the two electrons and the nucleus in the direction of the external magnetic field B_0. These transitions convert the LC into a level anti-crossing (LAC) (see Fig. 1). For instance, when we have an $S \leftrightarrow T_-$ LC, the HFC as perturbation makes an LAC from the $S\beta_N \leftrightarrow T_-\alpha_N$ crossing but does not affect the $S\alpha_N$ and $T_-\beta_N$ levels, which thus stay uncoupled to any other states. Hereafter, the subscript "N" denotes the nuclear spin state.

It was a challenging task in those days to analyze the involvement of the transient FAD biradical by means of magnetic resonance because of short relaxation times T_1 of the FAD protons. For studying CIDNP at variable magnetic field,

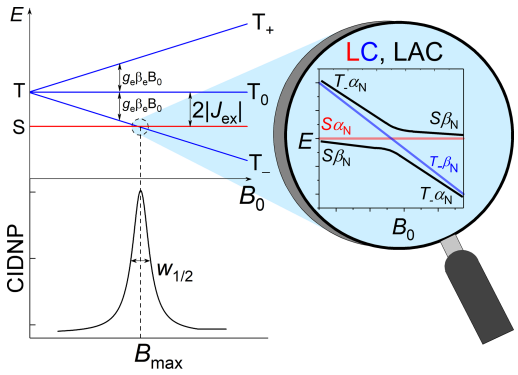

Figure 1. Energy levels diagram of a biradical or radical pair with negative exchange interaction and the level anti-crossing (LAC) mechanism explaining the resulting dependence of CIDNP on the magnetic field.

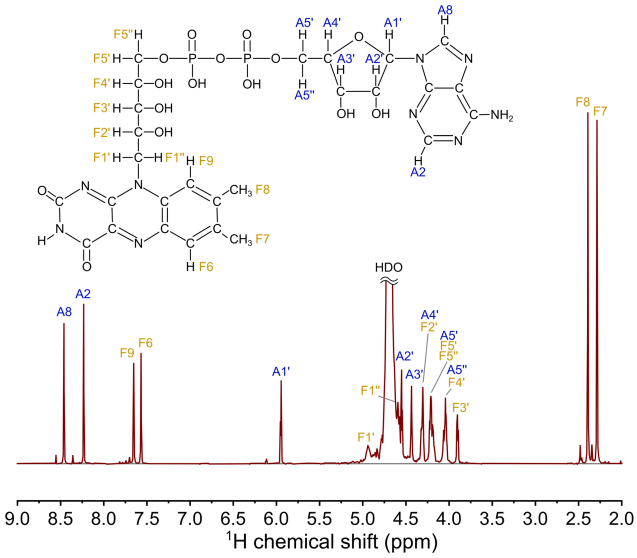

Figure 2. The 700 MHz ^{1}H NMR spectrum of 4.2 mM FAD solution in D_2O, pH 2.7, 25 °C.

a home-built falling-tube system was utilized, which allowed for sample transfer between two magnets, with one used for generation of the CIDNP effect and another one for its detection, but the transfer times were in conflict with T_1. The open question that stays even after more than 30 years is whether one or two biradicals with different inter-radical distances are actively contributing to CIDNP formation. In the meantime, the frontiers of nuclear hyperpolarization methods in general, and particularly the experimental tools for CIDNP detection were considerably improved, allowing us to get the answer to the question. Several milestones on that way date back to Robert Kaptein. The first milestone can be attributed to the introduction of time-resolved CIDNP with microsecond resolution detection for which he was among the pioneers (Hore and Kaptein, 1982). A second milestone was significant improvement of the fast field cycling technique, FFC, by introducing digitally controlled rapid mechanical shuttling of the NMR sample over an ultra-wide magnetic field range with high-resolution NMR detection (Zhukov et al., 2018). In our laboratory at the International Tomography Center (ITC) in Novosibirsk, we built up such a state-of-the-art mechanical shuttle device for available 400 and 700 NMR spectrometers. Such setups allow one to get site-specific information about molecular mobility with atomic resolution and to run CIDNP at variable magnetic field in a fully automatic way (Zhukov et al., 2020a, b). Last but not least, coherent transfer of hyperpolarization among scalar coupled spin as predicted by Kaptein (De Kanter and Kaptein, 1979) was firmly implemented into interpretation of CIDNP formed at low magnetic fields (Ivanov et al., 2008). Armed with these important improvements, we re-examine in the present paper the former CIDNP study of FAD with the aim to refine information on involvement of the adenine radical in the short-lived primary biradical of FAD and transformation of the biradical into the secondary FAD^-/Trp^+ radical pair by reductive electron transfer from tryptophan to the adenine radical moiety.

2 Materials and methods

Flavin adenine dinucleotide was kindly provided by Kiminori Maeda from Saitama University (Japan). D_2O (99.9 %) was purchased from Astrachem (Russia). The chemicals were used as received. The 700 MHz ^{1}H NMR spectrum of 4.2 mM FAD solution in D_2O, pH 2.7, and 25 °C, is shown in Fig. 2.

Nuclear magnetic relaxation dispersion (NMRD) experiments were run with 4.4 mM FAD solution in D_2O, pH 3.9, using a 700 MHz Bruker Avance III HD NMR spectrometer equipped with a TXI probe and a home-made fast field cycling add-on, similar to the one which has been built earlier (Zhukov et al., 2018). The 700 MHz add-on apparatus for mechanical shuttling and precise positioning of NMR samples inside the warm bore of the superconducting magnet closely resembles our other setup for the 400 MHz NMR spectrometer that was described previously (Zhukov et al., 2018). Details of the shuttling device for the 700 MHz NMR spectrometer will be published elsewhere.

The experimental protocol of the relaxation dispersion experiment is shown in Fig. 3a; it is similar to the protocol used to measure nuclear magnetic relaxation dispersion (NMRD) curves of ^{1}H and ^{13}C nuclei of methyl propiolate (Zhukov et al., 2018). The protocol consists of five stages: at the first stage nuclear spins relax to equilibrium in high field, B_0, then a 180° pulse is applied to invert spin magnetization. Next, the sample is transferred to a position along the magnet bore where the low field strength is equal to B_L. During the third stage the sample is kept in this field for a delay τ_{vd}. Then in the fourth stage the sample is shuttled back to the high field B_0, and after application of a hard 90° RF (radio frequency) pulse, the free induction decay (FID) is acquired. By repeat-

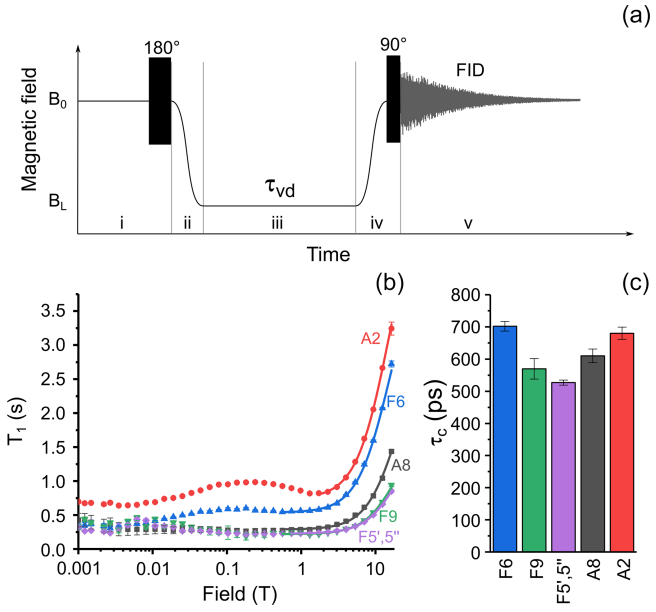

Figure 3. **(a)** Experimental protocol for measuring nuclear spin relaxation dispersion. In step (i), spins relax to thermal equilibrium at high field B_0, then a 180° RF pulse is applied for inversion of magnetization. In step (ii), the sample is transferred to the field B_L, where it is kept for an incremented delay τ_{vd} during step (iii). In step (iv), the sample is transferred back to high field B_0 and a 90° RF pulse is applied. In step (v), the nuclear spin free-induction decay is acquired, and the NMR spectrum is obtained after complex Fourier transform. **(b)** Relaxation dispersion data for six selected protons of FAD: A8 – black squares, A2 – red circles, F6 – blue up-pointing triangles, F5′,5″ – magenta diamonds, and F9 – green down-pointing triangles. Lines show best fit of high-field part of relaxation dispersion curves by Eq. (1). **(c)** Correlation times obtained from fitting the high-field part of relaxation dispersion data for protons A8; A2; F5′,5″; F6; and F9.

ing the cycle with systematically incrementing τ_{vd}, we obtain a series of 1D spectra with the corresponding delays τ_{vd} in field B_L. Although longitudinal relaxation of nuclear spins proceeds during the whole experimental cycle, the decay of signal intensity in the NMR spectra will depend merely on the duration of relaxation delay τ_{vd} but only if the field cycling is done with sufficient reproducibility. By analyzing the decay signal intensity with τ_{vd} for various low-field values B_L, one gets the NMRD curve – the magnetic field dependence of the longitudinal relaxation time T_1.

2.1 Chemically induced dynamic nuclear polarization in its dependence on the external magnetic field

CIDNP in its dependence on the external magnetic field was studied on a 400 MHz Bruker Avance III HD NMR spectrometer equipped with a fast-field-cycling unit and an add-on allowing for sample irradiation by compact LEDs (Zhukov et al., 2020a, 2018). A 4 mm diameter quartz rod is used as a light guide. It is inserted into the NMR sample tube so that its polished end is positioned just above the RF coil, when the sample is placed inside the NMR probe. A 520 nm 3 W LED with cooling radiator is attached to the other end of the light guide. The LED is turned on and off by an electro-mechanical relay controlled by transistor–transistor logic (TTL) pulses from the NMR spectrometer console in synchronization with the RF pulse sequence and the mechanical motion of the sample. To obtain CIDNP spectra, the experimental protocol depicted in Fig. 6a was used: at the first stage, sample magnetization relaxes at high field B_0 to its equilibrium value. Then, the sample is transferred to a position with the desired magnetic field strength B_L, where the LED is switched on for a fixed time interval $\tau_{irr} = 0.5$ s. Next, the sample is transferred back to the NMR probe at high field B_0 where the FID is acquired after application of a hard 90° RF pulse. For removal of thermal background polarization, two spectra are recorded: one with the LED being switched on at low field and the second one with the LED switched off. The difference between the two spectra gives the CIDNP spectrum. A typical CIDNP spectrum of the FAD sample at pH 2.7 detected at $B_L = 4$ mT is shown in Fig. 6b.

Since the sample transfer time in our 400 MHz setup is comparable with T_1 of FAD protons, it was necessary to reconstruct the real CIDNP field dependence by deconvolution of the observed CIDNP field dependence and the proton relaxation dispersion data. For this reconstruction, the computed dependence of the external magnetic field on time passed since transfer started (sample transfer time-field profile) $B_i \rightarrow B_0$ is divided into 500 intervals $\Delta t_n > 0$, for each field value B_i in the CIDNP field dependence. These intervals are counted decreasingly, so the first interval has number $n = 500$ and the last interval (just prior to FID acquisition) has number $n = 1$. For relaxation deconvolution purposes, the magnetic field B_n within each time interval was supposed to stay constant. Next, the measured nuclear spin relaxation dispersion curve is interpolated by cubic splines for all magnetic field values B_n, giving relaxation rates R_n for each interval. Finally, the true CIDNP intensity $P_{true}(i)$ generated in field B_i is reconstructed from the observed CIDNP intensity $P_{observed}(i)$ by the formula $P_{true}(i) = P_{observed}(i) \cdot \prod_{n=1}^{500} \exp(R_n \Delta t_n)$. The numerical simulation shows that approximately one-half of the A8 CIDNP signal is lost during sample transfer to high field.

2.2 Time-resolved (TR) CIDNP at high magnetic field

Our setup for TR-CIDNP measurements has already been described in detail (Morozova et al., 2007). The samples purged with pure nitrogen gas and sealed in a standard NMR Pyrex ampule were irradiated in the probe of a 200 MHz Bruker DPX-200 NMR spectrometer (magnetic field 4.7 T, resonance frequency of protons 200 MHz) by laser pulses from a Brilliant B Quantel Nd:YAG laser using its third har-

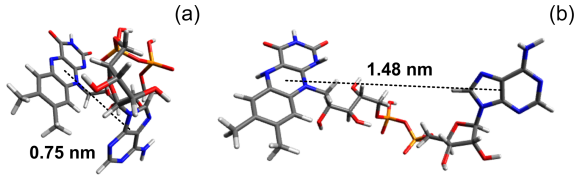

Figure 4. **(a)** Ground-state conformation of protonated FAD calculated in the Gaussian program package (Frisch et al., 2009). **(b)** Example of stretched FAD conformation (PDB ID fda; Bruns and Andrew, 1995; Berman et al., 2000). Pictures were made using Avogadro molecule visualizer (Hanwell et al., 2012).

monic (wavelength 355 nm, pulse length about 5 ns, output pulse energy 70–80 mJ). Light to the sample was guided using an optical system with a prism and a light-guide quartz rod (diameter 5 mm). The TR-CIDNP spectra were obtained in the following way: (1) saturation with broadband radio frequency pulses, (2) a 10 ns laser pulse triggered by the spectrometer, and (3) a detecting RF pulse of 1 µs duration followed by FID acquisition. The laser pulse was synchronized with the front edge of the RF pulse. As the background signals from Boltzmann polarization were suppressed by saturation pulses, in the CIDNP spectra only the NMR signals from the polarized products of the cyclic photochemical reaction appear.

3 Results and discussion

In a FAD molecule, the adenine and isoalloxazine rings are connected with each other by a long flexible ribityl phosphate linker; therefore, it is anticipated a priori that the FAD molecular structure in solution is likely to be represented by a number of conformations. As an example, two extreme cases of FAD conformations are shown in Fig. 4, with one of them being "closed" and the other one "open". The closed conformation was obtained in our density-functional theory (DFT) calculations of the 3D structure of a triplet excited FAD molecule in aqueous solution using the Gaussian program package (Frisch et al., 2009). Also, DFT calculations of IR spectra and FAD–water complex structure (Kieninger et al., 2020) have shown that the closed stacked conformation of FAD is stabilized by water molecules forming hydrogen bonds between adenine N7 in the purine ring and the ribityl chain. Another example of the extended open conformation was deduced from the analysis of X-ray diffraction data of the FAD–protein complex (PDB ID fda; Bruns and Andrew, 1995; Berman et al., 2000). Moreover, in the open conformation a hindered rotation might happen around the single bonds connecting the adenine ring to the ribose cycle and the isoalloxazine ring to the ribityl linker.

The obscured information about the preferable structure of FAD in aqueous solution is encoded by NMR in the correlation times of intramolecular mobility of individual protons and can be obtained from nuclear magnetic relaxation dispersion (NMRD), i.e., the dependence of the relaxation times on the magnetic field. With the aim to gain site-specific information about correlation times, we studied NMRD of protons with high spectral resolution over a wide range of magnetic fields, from 0.1 mT to 16.4 T.

For medium-sized molecules like FAD in water at room temperature, the transition between the fast and slow motional regimes, i.e., $\gamma_H B \tau_c \sim 1$, occurs in a field on the order of several tesla, which is manifested in a characteristic increase in the longitudinal relaxation time T_1. To get insight into the relative mobility of the adenine and isoalloxazine rings in solution, we analyzed the NMRD curves of all protons of FAD assuming a simple empirical model with two contributions to relaxation, one involving a site-specific local field correlation time τ_c^i and another one being a field-independent constant. Accordingly, the total relaxation rate is given by the sum $R_1^{\mathrm{tot}}(B) = \frac{R_1}{1+(\gamma_H B \tau_c)^2} + R_1^{\mathrm{inf}}$ and

$$T_1^i(B) = \frac{1 + \left(\gamma_H B \tau_c^i\right)^2}{R_1 + R_1^{\mathrm{inf}}\left(1 + \left(\gamma_H B \tau_c^i\right)^2\right)}, \quad (1)$$

where γ_H is the proton gyromagnetic ratio, τ_c^i the site-specific local field correlation time for ith proton, R_1 the site-specific local field relaxation rate in the fast motional regime $\gamma_H B \tau_c \ll 1$, and R_1^{inf} the magnetic field-independent relaxation rate. Since the dominant relaxation mechanism of protons is the modulation of dipole–dipole coupling, the τ_c^i values are expected to be close to each other for a molecule with rigid structure due to overall molecular tumbling; the deviation of τ_c^i from the average value highlights the molecular sites with increased or decreased mobility with respect to average. Lines in Fig. 3b show the best fit of FAD proton NMRD in the region from 0.56 to 16.44 T (1.77–16.44 T for A8 proton) by Eq. 1. The extracted correlation times are shown in Fig. 3c. The correlation times for protons in the isoalloxazine and adenine rings are alike, especially the ones of protons A8 and F6, meaning that no significant relative motions occur. Similar τ_c^i values were obtained for the protons of the linker. This observation supports conclusions drawn in recent quantum chemistry calculations of the FAD conformation in water (Kieninger et al., 2020), where a stacked conformation of the adenine and isoalloxazine rings was found in the FAD–water complex.

It is worth noting that only the "high field" part of the NMRD curve, which corresponds to the transition between the motional regimes, can be used to determine correlation times of individual protons with atomic resolution. In the "low field" part of NMRD where the extreme narrowing condition $\gamma_H B \tau_c \ll 1$ is met, the relaxation time of a particular spin cannot be obtained when spins are strongly coupled. Weak coupling means that the difference in resonance frequencies of a given nucleus i and other nucleus j, $|\Omega_i - \Omega_j|$, is larger than the scalar coupling $|J_{ij}|$ between them: $|\Omega_i - \Omega_j| \gg |J_{ij}|$; in the strong coupling of states,

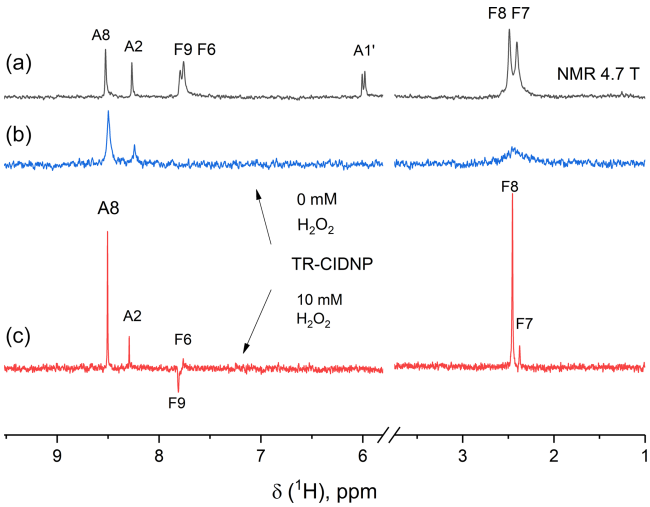

Figure 5. The 200 MHz NMR **(a)** and photo-CIDNP spectra **(b, c)** of a 0.9 mM solution of FAD in D_2O at pH 3.2 without H_2O_2 **(b)** and with 10 mM H_2O_2 **(c)** taken without delay after a short, single laser pulse. Background magnetization is removed by a saturation pulse sequence applied prior to the short, single laser pulse. Absorptive CIDNP signals are detected for the H8 and H2 protons of the adenine moiety in both CIDNP spectra, while for the flavin moiety absorptive signals of the F7- and F8-methyl protons and an emissive CIDNP signal of F9 are seen in the geminate spectrum obtained with addition of H_2O_2 **(c)**.

the inequality is opposite. It was shown previously by measuring proton relaxation dispersion of adenosine monophosphate (AMP) that A8 and A2 protons are strongly coupled (Kiryutin et al., 2016) at magnetic field below 10 mT, although their scalar coupling constant (0.25 Hz) was not observed by line splitting.

In the time-resolved CIDNP spectra (Fig. 5) of FAD in aqueous solution, obtained without delay after a short laser pulse of 10 ns with detection using an RF-pulse of 1 µs duration, signals from adenine and flavin are seen that have remarkably different linewidths. The absorptive lines of the adenine A8 and A2 protons are not as sharp as in the NMR spectrum. For flavin, only a very broad signal of low intensity is detected in the aliphatic part at the position of the methyl protons that we attributed to formation of the reduced flavin moiety, $FADH^-$. In contrast, in the spectrum obtained with addition of 10 mM of H_2O_2, all lines are as sharp as in the ordinary NMR spectrum, because addition of 10 mM hydrogen peroxide as a strong oxidizing agent significantly accelerates $FADH^-$ reoxidation to FAD. The absorptive signals of the F7- and F8-methyl protons as well as an emissive CIDNP signal of F9 are seen in the geminate spectrum. The sign of the CIDNP signals are in accordance with Kaptein's rule for triplet precursor multiplicity and a g factor of the flavin radical being larger than that of the adenine radical.

The most intense signal in the geminate ^{1}H CIDNP spectra is the A8 proton signal (Stob et al., 1989), highlighting that the largest spin density in the short-lived charge separated state of FAD is located on this proton. This observation is in agreement with the adenosine cation radical structure and the predicted isotropic hyperfine interaction constants: −0.57 mT for A8 and −0.32 mT for A2 (Adhikary et al., 2008). For short-lived radical pairs in a non-viscous solvent, proportionality between hyperfine coupling constants and geminate CIDNP signal intensities has been established (Morozova et al., 2011). We checked the proportionality of HFC constants and CIDNP for the A8 and A2 adenine protons of FAD (requiring CIDNP being zero for zero HFC) and found full agreement.

In the CIDNP spectra detected under continuous-wave (cw) illumination at low magnetic field, all signals are emissive (Fig. 6b). The position of the emissive maximum is common for adenine and flavin; the sign of polarization does not depend on the sign of HFC constants. This is in full accordance with the T_--S mechanism of CIDNP.

The main advantage of the fully automated setup for shuttling the sample is the possibility of fine-tuning the experimental conditions. As we noticed, the intensity ratio of the signals from A8 and A2 strongly depends on the irradiation time. This results from polarization transfer between them and different relaxation times. Since the HFC constant of A8 is larger than that of A2, we opted to measure the CIDNP field dependence of the A8 proton.

However, the relaxation dispersion measurements have shown a very short relaxation time of proton A8 (see Fig. 3b) at a magnetic field of 4 mT, which is optimal for CIDNP formation. In addition, in this field protons A8 and A2 are strongly coupled in the same way as it was shown for adenosine monophosphate (Kiryutin et al., 2016). Thus, measurement and analysis of field-dependent CIDNP of FAD protons should be done while taking into account these circumstances. Although their spin–spin coupling constant is small (below 0.4 Hz), comparable with the linewidths of adenine, and is not seen as a splitting, the low magnetic field gives rise to strong coupling between protons A8 and A2 in FAD and thus leads to coherent transfer of light-induced proton hyperpolarization between them. Since proton A2 has a more than 2 times longer T_1, this proton shows a higher CIDNP effect in comparison to A8 when irradiation time τ_{irr} is 2–3 s. To avoid polarization transfer, we used a short irradiation time ($\tau_{irr} = 0.5$ s), which is long enough for A8 to reach its steady-state polarization level but sufficiently short to keep the share of polarization leaked to A2 relatively small. With such optimized settings, we measured proton CIDNP field dependences of FAD samples at pH 2.7 and pH 3.9. These measured CIDNP field dependences were corrected to the genuine CIDNP field dependence using the relevant nuclear spin relaxation dispersion data and the time profile of the sample transfer. No difference between A8 CIDNP field dependences was found within experimental error except for a fourfold decrease in CIDNP intensity when the pH was

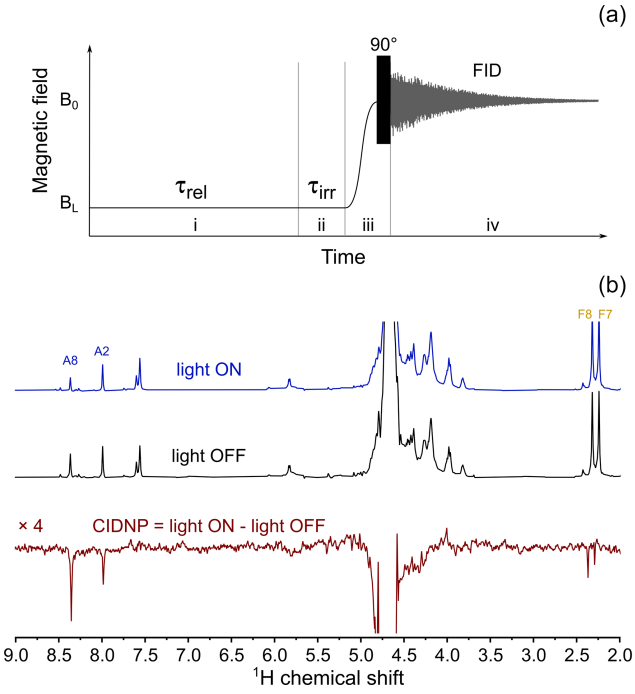

Figure 6. **(a)** Experimental protocol for measuring the CIDNP field dependence. In stage (i) the sample relaxes in low field, B_L, for $\tau_{rel} = 5$ s. Then, in stage (ii) the LED is either switched on (in "light ON" experiment) or stays switched off (in "light OFF" experiment) for $\tau_{irr} = 0.5$ s. In stage (iii) the sample is transferred to high field, B_0, and a 90° RF pulse is applied. In stage (iv) nuclear spin free-induction decay is acquired. **(b)** Top spectrum: 400 MHz ^{1}H NMR spectrum obtained using the protocol shown in panel **(a)**, with 3 W 520 nm LED switched on during stage (ii) of the protocol, $B_L = 4$ mT; middle spectrum: 400 MHz ^{1}H NMR spectrum obtained using the protocol shown in panel **(a)**, LED is switched off during stage (ii) of the protocol, $B_L = 4$ mT; bottom spectrum: $B_L = 4$ mT CIDNP spectrum which is the difference between "light ON" and "light OFF" spectra taken in this field.

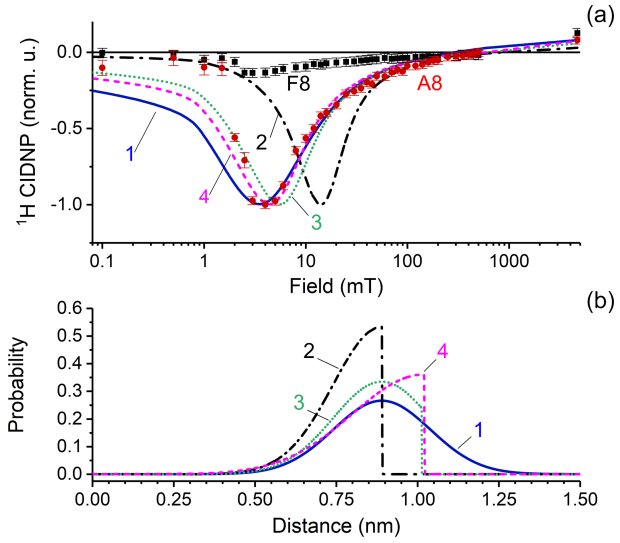

Figure 7. **(a)** CIDNP dependence on the magnetic field. Red circles and black squares represent experimental data for adenine A8 and flavin F8 protons; CIDNP data corrected by taking into account nuclear relaxation occurring during sample transfer to the detection position at high field. Lines show the numerical simulation of CIDNP field dependences with the parameters listed in Table 1, using four different distance distribution functions which are depicted in panel **(b)**. The fit quality is characterized by the q value that is the sum of squared deviations from the experimentally observed data. The q values are 1.8×10^{-3}, 9×10^{-3}, 5.2×10^{-3}, and 3.9×10^{-3} for simulations 1–4, respectively. **(b)** Model biradical end-to-end distribution functions used for simulations of the CIDNP field dependence: simulation 1 (blue solid line) – normal distribution centered at 0.89 nm with standard deviation 0.15 nm; simulation 2 (black dashed-dotted line) – left half of normal distribution centered at 0.89 nm with standard deviation 0.15 nm; simulation 3 (green dotted line) – normal distribution centered at 0.89 nm with standard deviation 0.15 nm, with distances above 1.03 nm cut; and simulation 4 (magenta dashed line) – left half of normal distribution centered at 10.2 nm with standard deviation 0.22 nm.

changed from 2.7 to 3.9. Further pH increase leads to diminishing CIDNP.

The CIDNP data for proton A8 are shown in Fig. 7a by red circles. A well-pronounced single maximum is detected in the wide range of magnetic fields between 0.1 mT and 9.4 T. The high quality of the data left no doubts that only one maximum of CIDNP is detected in the field dependence, excluding the fact that two types of biradical with different exchange interactions are formed from FAD. The maximum is located at 4 mT, and the full width of the maximum is about 10 mT.

To get more detailed information about the structure and exchange interaction in the FAD biradical, we simulated the CIDNP field dependence using the approach originally proposed in the work of Kaptein and co-authors (de Kanter et al., 1977) for calculating CIDNP in flexible biradicals. This model was widely used in our studies of CIDNP in cyclic aliphatic ketones (Tsentalovich et al., 2002; Yurkovskaya et al., 1995; Morozova et al., 1997a, b; Tsentalovich et al., 1997) and the model compound containing flavin and tryptophan connected by a polymethylene chain (Paul et al., 2017).

The position of the CIDNP maximum and the shape of the simulated CIDNP field dependence strongly depend on the radial distribution function chosen. Simulation parameters are listed in Table 1. Based on both theoretical and experimental evidence of closed and rigid structures of FAD in aqueous solution, we assume that the light-induced biradical state of FAD conserves these properties to a large extent. We tested several model functions of radial distribution and found the best correspondence between simulation and experiment for a normal distribution, centered at $r_0 = 0.89$ nm, with standard deviation $\sigma = 0.15$ nm. We also tried other end-to-end distribution functions for simulation of CIDNP field dependences. The results are shown in Fig. 7. Simu-

Table 1. Parameters used to model the CIDNP field dependence.

Symbol	Description	Value
g_a	g factor of the first radical (adenine)	2.0034
A	hyperfine interaction constant on spin-1/2 nuclei to be observed	−0.7 mT
g_b	g factor of the second radical (flavin)	2.0035
J_0	amplitude parameter of exchange interaction, $J_{ex}(r) = J_0 \cdot e^{-\alpha r}$	-2.3×10^8 mT
α	exchange interaction distance decay parameter	0.214 nm
D	effective radial diffusion coefficient in biradical state	2×10^{-7} cm^2 s^{-1}
G	mean-square fluctuating local field	6.1×10^{17} s^{-2}
τ_u	local field correlation time	1 ps
τ_{rot}	rotational diffusion correlation time	800 ps
k_p	recombination rate constant from singlet state	2×10^{10} s^{-1}
k_s	scavenging rate to minor reaction products	10^5 s^{-1}
A_{add}	hyperfine interaction constant with additional spin-1/2 nuclei	1.67 mT
n	number of additional nuclei	4

lation 1 (blue solid line) – normal distribution centered at 0.89 nm with a standard deviation of 0.15 nm; simulation 2 (black dashed-dotted line) – left half of a normal distribution centered at 0.89 nm with standard deviation of 0.15 nm; simulation 3 (green dotted line) – normal distribution centered at 0.89 nm with standard deviation of 0.15 nm, but distances above 1.03 nm are cut; simulation 4 (magenta dashed line) – left half of a normal distribution centered at 10.2 nm with a standard deviation of 0.22 nm. The fit quality is characterized by the q value that is the sum of squared deviations from the experimentally observed data which are 1.8×10^{-3}, 9×10^{-3}, 5.2×10^{-3} and 3.9×10^{-3} for simulations 1–4, respectively. Thus we conclude that the best function is a normal distribution centered at 0.89 nm with a standard deviation of 0.15 nm.

We also preliminarily examined samples containing FAD with addition of tryptophan at variable concentration. For low tryptophan concentration, the emissive maximum at low field stayed at its position around 4 mT for flavin and adenine protons, while at the high field polarization of tryptophan was observed. It is a clear indication that the spin evolution of the biradical has an influence on the overall magnetic field dependence of the flavin radical in the primary biradical and in the secondary radical pair where spins are not correlated. We detected a remarkably different dependence of CIDNP for flavin and tryptophan under variation of the tryptophan concentration, but a detailed discussion is beyond the scope of the present paper. This work is underway in our laboratories, and the results will be published elsewhere.

4 Conclusions

In this study we measured and analyzed the magnetic field dependence of ^{1}H CIDNP to confirm the involvement of the adenine radical in the primary photochemical reaction of intramolecular electron transfer in FAD, resulting in formation of the flavin–adenine biradical. By reducing the light irradiation time to 0.5 s for CIDNP formation at low magnetic field, we avoided coherent polarization transfer among the protons of adenine and obtained for the A8 proton a magnetic field dependence with a single emissive maximum located at 4 mT. A dependence of the same shape was detected for the methyl protons of flavin. The dependence of relaxation times T_1 on the magnetic field between 1 and 16 T allowed us to determine the correlation times, τ_c, of intramolecular mobility with atomic resolution. From the coincidence of τ_c for the protons of flavin and adenine and the absence of any short correlation times (but there is $\tau_u = 1$ ps), we conclude that the structure of the FAD molecule is rigid. Modeling of the CIDNP field dependence in the frame of the model proposed by Kaptein provides good agreement with the experimental data for a normal distance distribution between the two radical centers of 0.89 nm with a standard deviation of 0.15 nm. Time-resolved CIDNP spectra recorded without delay between the short laser excitation pulse and detection confirmed that back electron transfer leads to formation of a diamagnetic adenine and reduced flavin of $FADH^-$, whereas with addition of oxidizing agent H_2O_2 the diamagnetic FAD is restored on the geminate stage.

Code availability. CIDNP simulation program and Fortran source code are available at https://doi.org/10.5281/zenodo.4680150 (Lukzen and Ivanov, 2021).

Data availability. The data used for generating Figs. 3, 6, and 7 can be found at https://doi.org/10.5281/zenodo.4680209 (Zhukov et al., 2021).

Author contributions. AVY and HMV designed the project. IVZ and NNF conducted the CIDNP experiments, and ASK measured

the proton nuclear relaxation dispersion. MSP performed the quantum chemistry calculations. NNL and KLI wrote the CIDNP simulation code. IVZ conducted the numerical simulations of the CIDNP field dependence. IVZ, NNF, OBM, HMV, RZS, and AVY analyzed the results. All authors contributed to article preparation.

Competing interests. The authors declare that they have no conflict of interest.

Special issue statement. This article is part of the special issue "Robert Kaptein Festschrift". It is not associated with a conference.

Acknowledgements. The authors are grateful to the Russian Science Foundation (RSF), the Russian Foundation for Basic Research and Deutsche Forschungsgemeinschaft (RFBR-DFG) for financial support.

Financial support. The experimental part of this research has been supported by RSF (grant no. 20-63-46034) and the theoretical part has received joint support from the RFBR-DFG (grant no. 21-53-12023).

Review statement. This paper was edited by Rolf Boelens and reviewed by Peter Hore and one anonymous referee.

References

Adhikary, A., Kumar, A., Khanduri, D., and Sevilla, M. D.: Effect of Base Stacking on the Acid-Base Properties of the Adenine Cation Radical [$A^{\bullet+}$] in Solution: ESR and DFT Studies, J. Am. Chem. Soc., 130, 10282–10292, https://doi.org/10.1021/ja802122s, 2008.

Ahmad, M.: Photocycle and Signaling Mechanisms of Plant Cryptochromes, Curr. Opin. Plant Biol., 33, 108–115, https://doi.org/10.1016/j.pbi.2016.06.013, 2016.

Antill, L. M. and Woodward, J. R.: Flavin adenine dinucleotide photochemistry is magnetic field sensitive at physiological pH, J. Phys. Chem. Lett., 9, 26910–2696, https://doi.org/10.1021/acs.jpclett.8b01088, 2018.

Berman, H. M., Westbrook, J., Feng, Z., Gilliland, G., Bhat, T. N., Weissig, H., Shindyalov, I. N., and Bourne, P. E.: The Protein Data Bank, Nucleic Acids Res., 28, 235–242, https://doi.org/10.1093/nar/28.1.235, 2000.

Bruns, C. M. K. and Andrew, P.: Refined Crystal Structure of Spinach Ferredoxin Reductase at 1.7 Å Resolution: Oxidized, Reduced and 2′-Phospho-5′-AMP Bound States, J. Mol. Biol., 247, 125–145, https://doi.org/10.1006/jmbi.1994.0127, 1995.

De Kanter, F. J. J. and Kaptein, R.: CIDNP Transfer Via Nuclear Dipolar Relaxation and Spin-Spin Coupling, Chem. Phys. Lett., 62, 421–426, https://doi.org/10.1016/0009-2614(79)80733-2, 1979.

de Kanter, F. J. J., den Hollander, J. A., Huizer, A. H., and Kaptein, R.: Biradical CIDNP and the Dynamics of Polymethylene Chains, Mol. Phys., 34, 857–874, https://doi.org/10.1080/00268977700102161, 1977.

Dodson, C. A., Wedge, C. J., Murakami, M., Maeda, K., Wallace, M. I., and Hore, P. J.: Fluorescence-detected magnetic field effects on radical pair reactions from femtolitre volumes, Chem. Commun., 51, 8023–8026, https://doi.org/10.1039/C5CC01099C, 2015.

Frisch, M. J., Trucks, G. W., Schlegel, H. B., Scuseria, G. E., Robb, M. A., Cheeseman, J. R., Scalmani, G., Barone, V., Petersson, G. A., Nakatsuji, H., X. Li, M. C., Marenich, A., Bloino, J., Janesko, B. G., Gomperts, R., Mennucci, B., Hratchian, H. P., Ortiz, J. V., Izmaylov, A. F., Sonnenberg, J. L., Williams-Young, D., Ding, F., Lipparini, F., Egidi, F., Goings, J., Peng, B., Petrone, A., Henderson, T., Ranasinghe, D., Zakrzewski, V. G., Gao, J., Rega, N., Zheng, G., Liang, W., Hada, M., Ehara, M., Toyota, K., Fukuda, R., Hasegawa, J., Ishida, M., Nakajima, T., Honda, Y., Kitao, O., Nakai, H., Vreven, T., Throssell, K., Jr., J. A. M., Peralta, J. E., Ogliaro, F., Bearpark, M., Heyd, J. J., Brothers, E., Kudin, K. N., Staroverov, V. N., Keith, T., Kobayashi, R., Normand, J., Raghavachari, K., Rendell, A., Burant, J. C., Iyengar, S. S., Tomasi, J., Cossi, M., Millam, J. M., Klene, M., Adamo, C., Cammi, R., Ochterski, J. W., Martin, R. L., Morokuma, K., Farkas, O., Foresman, J. B., and Fox, D. J.: Gaussian 09, Revision A.02, Gaussian, Inc., Wallingford, CT, USA, 2009.

Hanwell, M. D., Curtis, D. E., Lonie, D. C., Vandermeersch, T., Zurek, E., and Hutchison, G. R.: Avogadro: An Advanced Semantic Chemical Editor, Visualization, and Analysis Platform, J. Cheminformatics, 4, 17, https://doi.org/10.1186/1758-2946-4-17, 2012.

Hore, P. J. and Kaptein, R.: Photochemically Induced Dynamic Nuclear-Polarization (Photo-CIDNP) of Biological Molecules Using Continuous Wave and Time-Resolved Methods, ACS Symp. Ser., 191, 285–318, 1982.

Hore, P. J. and Mouritsen, H.: The Radical-Pair Mechanism of Magnetoreception, Ann. Rev. Biophys., 45, 299–344, https://doi.org/10.1146/annurev-biophys-032116-094545, 2016.

Ivanov, K. L., Yurkovskaya, A. V., and Vieth, H.-M.: Coherent Transfer of Hyperpolarization in Coupled Spin Systems at Variable Magnetic Field, J. Chem. Phys., 128, 154701, https://doi.org/10.1063/1.2901019, 2008.

Kieninger, M., Ventura, O. N., and Kottke, T.: Calculation of the Geometries and Infrared Spectra of the Stacked Cofactor Flavin Adenine Dinucleotide (FAD) as the Prerequisite for Studies of Light-Triggered Proton and Electron Transfer, Biomolecules, 10, 573, https://doi.org/10.3390/biom10040573, 2020.

Kiryutin, A. S., Pravdivtsev, A. N., Ivanov, K. L., Grishin, Y. A., Vieth, H.-M., and Yurkovskaya, A. V.: A Fast Field-Cycling Device for High-Resolution NMR: Design and Application to Spin Relaxation and Hyperpolarization Experiments, J. Magn. Reson., 263, 79–91, https://doi.org/10.1016/j.jmr.2015.11.017, 2016.

Lukzen, N. and Ivanov, K.: CIDNP field dependence simulation program for flexible biradicals. Magnetic Resonance, Zenodo, https://doi.org/10.5281/zenodo.4680150, 2021.

Morozova, O. B., Yurkovskaya, A. V., Tsentalovich, Y. P., Sagdeev, R. Z., Wu, T., and Forbes, M. D. E.: Study of Consecutive Biradicals from 2-Hydroxy-2,12-Dimethylcyclododecanone by TR-CIDNP, TREPR, and Laser Flash Photolysis, J. Phys. Chem. A, 101, 8803–8808, https://doi.org/10.1021/jp9711196, 1997a.

Morozova, O. B., Yurkovskaya, A. V., Tsentalovich, Y. P., and Vieth, H.-M.: ^{1}H and ^{13}C Nuclear Polarization in Consecutive Biradicals During the Photolysis of 2,2,12,12-Tetramethylcyclododecanone, J. Phys. Chem. A, 101, 399–406, https://doi.org/10.1021/jp961456z, 1997b.

Morozova, O. B., Kiryutin, A. S., Sagdeev, R. Z., and Yurkovskaya, A. V.: Electron Transfer between Guanosine Radical and Amino Acids in Aqueous Solution. 1. Reduction of Guanosine Radical by Tyrosine, J. Phys. Chem. B, 111, 7439–7448, 2007.

Morozova, O. B., Ivanov, K. L., Kiryutin, A. S., Sagdeev, R. Z., Köchling, T., Vieth, H.-M., and Yurkovskaya, A. V.: Time-Resolved CIDNP: An NMR Way to Determine the EPR Parameters of Elusive Radicals, Phys. Chem. Chem. Phys., 13, 6619–6627, https://doi.org/10.1007/BF03166215, 2011.

Murakami, M., Maeda, K., and T. Arai.: Dynamics of intramolecular electron transfer reaction of FAD studied by magnetic field effects on transient absorption spectra, J. Phys. Chem. A., 109, 5793–5800, https://doi.org/10.1021/jp0519722, 2005.

Paul, S., Kiryutin, A. S., Guo, J., Ivanov, K. L., Matysik, J., Yurkovskaya, A. V., and Wang, X.: Magnetic Field Effect in Natural Cryptochrome Explored with Model Compound, Sci. Rep., 7, 11892, https://doi.org/10.1038/s41598-017-10356-4, 2017.

Stob, S., Kemmink, J., and Kaptein, R.: Intramolecular Electron Transfer in Flavin Adenine Dinucleotide. Photochemically Induced Dynamic Nuclear Polarization Study at High and Low Magnetic Fields, J. Am. Chem. Soc., 111, 7036–7042, 1989.

Tsentalovich, Y. P., Morozova, O. B., Avdievich, N. I., Ananchenko, G. S., Yurkovskaya, A. V., Ball, J. D., and Forbes, M. D. E.: Influence of Molecular Structure on the Rate of Intersystem Crossing in Flexible Biradicals, J. Phys. Chem. A, 101, 8809–8816, https://doi.org/10.1021/jp972717n, 1997.

Tsentalovich, Y. P., Forbes, M. D. E., Morozova, O. B., Plotnikov, I. A., McCaffrey, V. P., and Yurkovskaya, A. V.: Spin and Molecular Dynamics in Acyl-Containing Biradicals: Time-Resolved Electron Paramagnetic Resonance and Laser Flash Photolysis Study, J. Phys. Chem. A, 106, 7121–7129, https://doi.org/10.1021/jp020098z, 2002.

Wiltschko, R. and Wiltschko, W.: Magnetoreception in Birds, J. R. Soc. Interface, 16, 20190295, https://doi.org/10.1098/rsif.2019.0295, 2019.

Yurkovskaya, A. V., Morozova, O. B., Sagdeev, R. Z., Dvinskih, S. V., Buntkowsky, G., and Vieth, H.-M.: The Influence of Scavenging on CIDNP Field Dependences in Biradicals During the Photolysis of Large-Ring Cycloalkanones, Chem. Phys., 197, 157–166, https://doi.org/10.1016/0301-0104(95)00125-8, 1995.

Zhukov, I. V., Kiryutin, A. S., Yurkovskaya, A. V., Grishin, Y. A., Vieth, H.-M., and Ivanov, K. L.: Field-Cycling NMR Experiments in Ultra-Wide Magnetic Field Range: Relaxation and Coherent Polarization Transfer, Phys. Chem. Chem. Phys., 20, 12396–12405, https://doi.org/10.1039/C7CP08529J, 2018.

Zhukov, I., Fishman, N., Kiryutin, A., Lukzen, N., Panov, M., Steiner, U., Vieth, H.-M., Schäfer, J., Lambert, C., and Yurkovskaya, A.: Positive Electronic Exchange Interaction and Predominance of Minor Triplet Channel in CIDNP Formation in Short Lived Charge Separated States of D-X-A Dyads, J. Chem. Phys, 152, 014203, https://doi.org/10.1063/1.5131817, 2020a.

Zhukov, I. V., Kiryutin, A. S., Ferrage, F., Buntkowsky, G., Yurkovskaya, A. V., and Ivanov, K. L.: Total Correlation Spectroscopy across All NMR-Active Nuclei by Mixing at Zero Field, J. Phys. Chem. Lett., 11, 7291–7296, https://doi.org/10.1021/acs.jpclett.0c02032, 2020b.

Zhukov, I. V., Kiryutin, A. S., Panov, M. S., Fishman, N. N., Morozova, O. B., Lukzen, N. N., Ivanov, K. L., Vieth, H.-M., Sagdeev, R. Z., and Yurkovskaya, A. V.: Data for "Exchange interaction in FAD biradical", Magnetic Resonance, 2, 2021 [Data set]. Magnetic Resonance, Zenodo, https://doi.org/10.5281/zenodo.4680209, 2021.